

New well architectures assessment for geothermal exploitation of the Triassic sandstones in Paris basin

Virginie Hamm, Madjid Bouzit, Simon Lopez

▶ **To cite this version:**

Virginie Hamm, Madjid Bouzit, Simon Lopez. New well architectures assessment for geothermal exploitation of the Triassic sandstones in Paris basin. European Geothermal Congress : EGC 2016, Sep 2016, Strasbourg, France. hal-01340399

HAL Id: hal-01340399
https://brgm.hal.science/hal-01340399

Submitted on 1 Jul 2016

HAL is a multi-disciplinary open access archive for the deposit and dissemination of scientific research documents, whether they are published or not. The documents may come from teaching and research institutions in France or abroad, or from public or private research centers.

L'archive ouverte pluridisciplinaire **HAL**, est destinée au dépôt et à la diffusion de documents scientifiques de niveau recherche, publiés ou non, émanant des établissements d'enseignement et de recherche français ou étrangers, des laboratoires publics ou privés.

New well architectures assessment for geothermal exploitation of the Triassic sandstones in Paris basin

Virginie Hamm[1], Madjid Bouzit[1], Simon Lopez[1].

[1] BRGM, 3 av. Claude Guillemin, 45060 Orléans Cedex 2, France

Corresponding author: v.hamm@brgm.fr

Keywords: Paris basin, Triassic sandstones, geothermal well architectures, doublet performance, modelling analysis, cost performance analysis.

ABSTRACT

The deep geothermal resource of the center of the Paris basin (Ile-de-France, France) has been exploited since the mid-1980s, the main target being the Dogger limestone aquifer (1,500–2,000 m deep, 55–80°C). Currently, the Triassic sandstone units below the Dogger aquifer are envisaged as new targets. This paper presents a modelling and economic analysis used to assess new well architectures (sub-horizontal, horizontal or multilateral wells) in comparison with standard geothermal operation, with a view to increasing doublet hydraulic performance and to enable the exploitation of the Triassic sandstones with lower permeabilities compared to the Dogger aquifer. The results of the modelling analysis are expressed in terms of a doublet performance index (DPI, in m3/(h.bar)), which is the average between the productivity and injectivity indices. Economic analysis results are given in terms of a doublet cost-performance index (CPI, in k€/year/DPI). The results suggest that both DPI and CPI are better for complex well architectures compared to standard deviated wells. The extra costs of complex well architectures compared to the cost of standard wells are largely offset by the relative benefits of increasing doublet hydraulic performance. However, improvements in drilling technologies and further experience from new operations will lead to substantial cost reductions in the future.

1. INTRODUCTION

The Triassic sandstone units underlying the Dogger aquifer (Fig. 1) have good reservoir properties and may constitute attractive geothermal targets for district heating. Attempts at their geothermal exploitation were made in the early 1980s (Boisdet at al, 1989; Lopez et Millot, 2008) but these proved unsuccessful: the deep layers proved hotter but less productive than the overlying Dogger aquifer. Out of the three projects targeting this formation, only one – the Melleray facility located in the south-western part of the sedimentary basin – was commissioned; it ran for no more than a year in the face of injection related problems.

However, deep Triassic aquifers in the Paris basin – at depths of between 2,000 and 2,500 m and with temperatures up to 120°C in some areas – are now considered a possible target for power production and heat cogeneration. The main difficulties to be overcome in exploitation of the Triassic sandstones relate to the nature of the aquifer, which consists of fluvial deposits with permeable sand bodies that are relatively narrow and disconnected. Its properties (i.e. porosity and permeability) are thus more heterogeneous and discontinuous than those of the Dogger limestone aquifer. Permeability can vary by a factor of over one thousand between sandy facies and more impervious ones (Eschard et al., 1998). Recent work has allowed better characterizing of the Triassic geothermal reservoirs of the Paris basin (Bouchot et al, 2012) and of the impact of fluvial sedimentary heterogeneities on a geothermal doublet (Hamm and Lopez, 2012). Nevertheless, if exploitation failure is to be avoided, further investigations are required before drilling of new wells in the Triassic aquifer.

The main objective of this paper is to quantify the impact of well trajectories / paths inside the reservoir on the performance and cost of geothermal doublet. In chapter 2, we lay out the model and its specifications and discuss modelling results. In chapter 3, we provide some clues on cost-performance analysis.

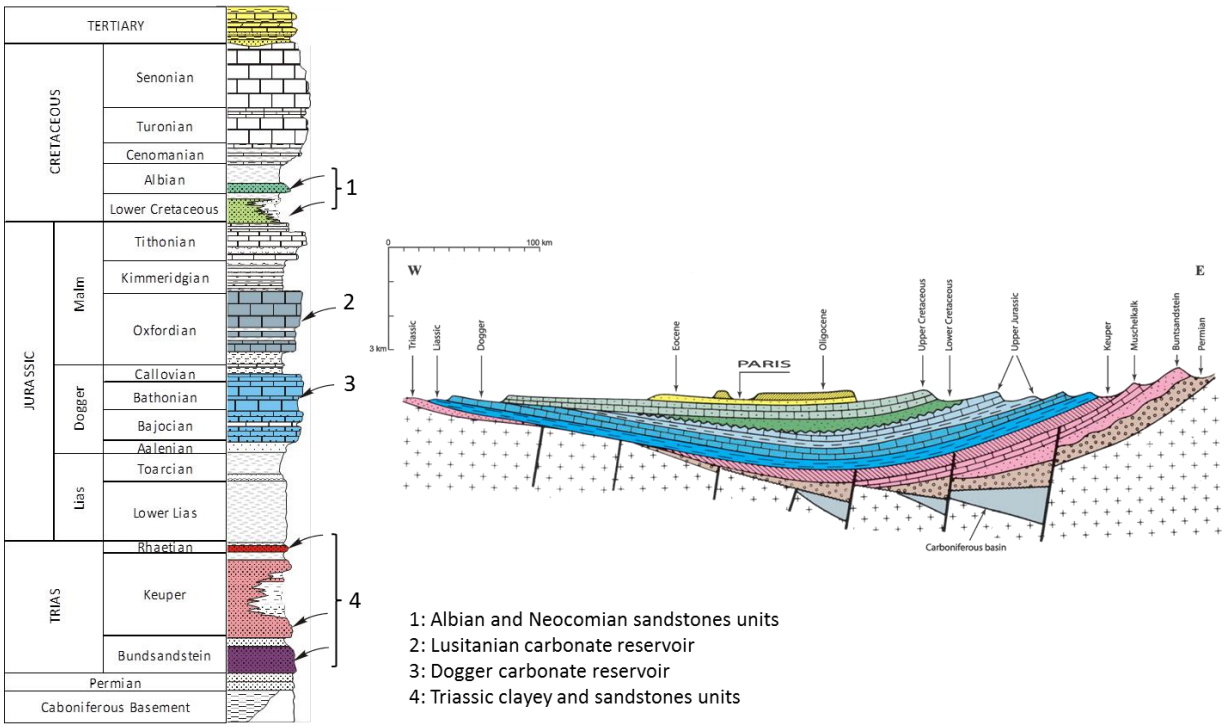


Figure 1: Triassic sandstone units in Paris basin

2. MODELING ANALYSIS

2.1 Methodology

Numerous examples of work can be found in the literature on the development and application of wellbore models coupled to reservoir models (Hadgu et al, 1995; Amara et al, 2008; Remoroza et al, 2011; Pan et al, 2013, 2015; Saeid at al, 2013, 2014). Hadgu et al., Remoroza et al. and Pan et al. used the TOUGH2 finite difference code for 3D reservoir modelling coupled to wellbore models (WSFA, T2Well) to simulate non-isothermal, single-phase or two-phase, steady-state or transient flow in a wellbore reservoir system. Saeid et al. developed a 1D-2D wellbore-reservoir model using the COMSOL finite element code describing the coupling between heat transfer in the well, the reservoir and the host rock.

We propose here an integrated 1D-3D wellbore-reservoir flow model using the COMSOL Multiphysics software. The Darcian flow in the 3D reservoir is coupled with the wellbore flow which is modelled by a pseudo 1D momentum equation describing the conservation of the fluid displacement at each well (producer and injector). This formula allows description of the flow and pressures in the well without the need for complex 3D discretization for the well, as it requires only one-dimensional elements coupled to the 3D reservoir geometry. For heat transfer, we applied a Dirichlet boundary condition with constant temperature at the injection well and an outflow boundary condition at the production well. Because we focus on the interaction between well architecture and the reservoir, we consider only the part of the well intercepting the reservoir and not the part between the top of the reservoir and the wellhead. The mathematical developments are given in Appendix A (nomenclature), Appendix B (governing equation for 1D wellbore flow model and 3D porous model) and Appendix C (boundary and initial conditions).

This coupled wellbore-reservoir model was applied to different well architectures (slightly deviated wells, highly deviated to horizontal wells or multilateral wells), described in Section 2.2, and we calculated the corresponding productivity and injectivity index of each well (injector and producer).

2.2 Model description and modelling cases

In the oil industry, accurate description of sedimentary heterogeneities is a key aspect of reservoir characterization, as they may have a significant impact on dynamic processes such as water flooding and oil recovery (e.g. Pranter et al., 2007). Static reservoir modelling relies most often on geostatistical techniques to directly reproduce the distribution of the parameters of interest (lithofacies, petrophysical properties) based on estimates from spatial statistics and on the choice of an appropriate probabilistic model. Two different types of methods can be distinguished: (i) pixel based methods, where a continuous function is evaluated on a discrete grid; and (ii) boolean methods that consist in throwing randomly discrete objects into space. As both types of methods can be used to produce conditional simulation respecting well constraints, they are used intensively for practical purposes (e.g. Chilès & Delfiner, 1999).

For Triassic sandstones, the model uses a static 3D numerical grid produced by a combined stochastic and process-based approach considered to be representative of a realistic sedimentary architecture (Lopez, 2003; Lopez et al., 2008) and which has been successfully tested by several oil companies. The numerical block is 10 km long, 8 km wide and 50 m thick. The permeability distribution was introduced into the COMSOL Multiphysics model via an interpolation function. Nine lithofacies were used to represent the sedimentary deposits and exported in a regular grid with a 100 m horizontal spacing and 2 m vertical spacing. A view of the lithofacies block in the COMSOL model is shown in Fig. 2. In order to represent the Trias fluviatile series for the Paris basin, different horizontal and vertical permeabilities have been assigned to each of the lithofacies, using data from the literature on the Chaunoy oil field (Eschard et al., 1998; Hamm et Lopez, 2012). For heat transfer, an average thermal conductivity and heat capacity were chosen from amongst usual values for sedimentary deposits. Table 1 lists petrophysical property values assigned to each of the lithofacies.

Table 1: Different lithofacies and petrophysical values

Lithofacies	Porosity (%)	Horizontal permeability (mD)	Vertical permeability (mD)
Channel lag	15	400	400
Sand plug	10	50	1
Point bar	8	400	5
Crevasse splay I	12	80	80
Crevasse splay II channels	8	50	1
Crevasse splay II	20	1	0.1
Mud plug	20	0.1	0.01
Overbank alluvium	20	0.2	0.02
Levee	12	1	0.1

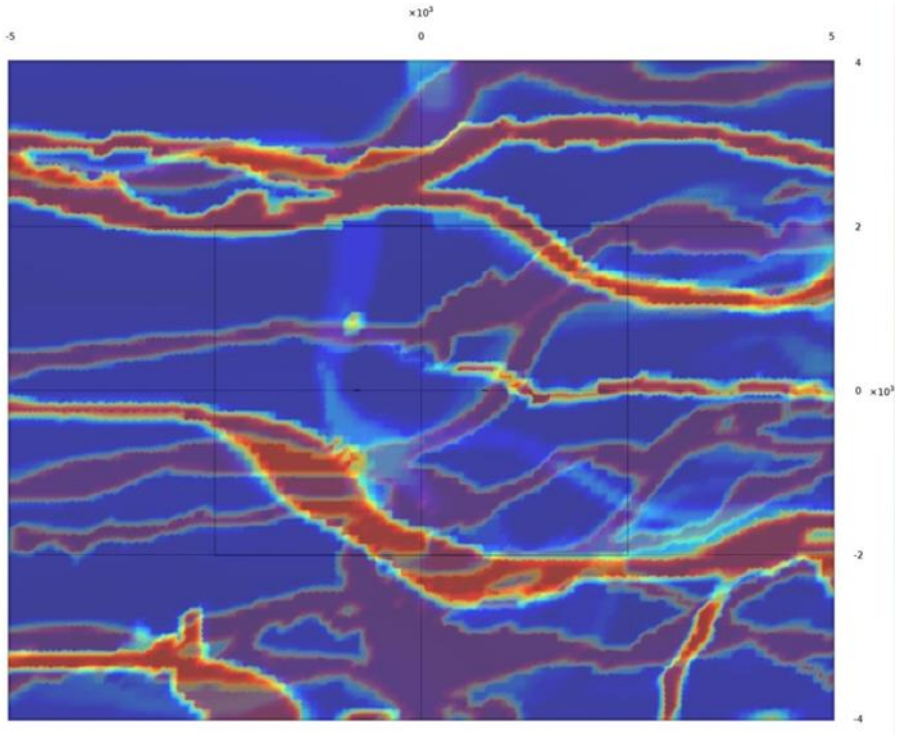


Figure 2: 3D permeability model of fluvial deposits (red: more permeable lithofacies, blue: more impervious lithofacies).

To benchmark well architectures in terms of both hydraulic performance and costs, five cases were defined and used in the simulations, and for economic analysis (Fig. 3). The simulation was conducted for a set of comparable geological conditions and with identical completion well diameter. On average, the true vertical depth (TVD) is 2,250 m for Trias reservoirs. The total drilled depth (TDD) was calculated on the basis of a fixed distance of 1.5 km between the two well impacts at the top reservoir (common average distance between geothermal wells), and for a reservoir thickness of 50 m. TDD is the total distance drilled as measured along deviated production or injection wells, including the total length of drains, i.e. part of the well intercepting reservoirs. TVD and TDD for the five cases are given in Table 2.

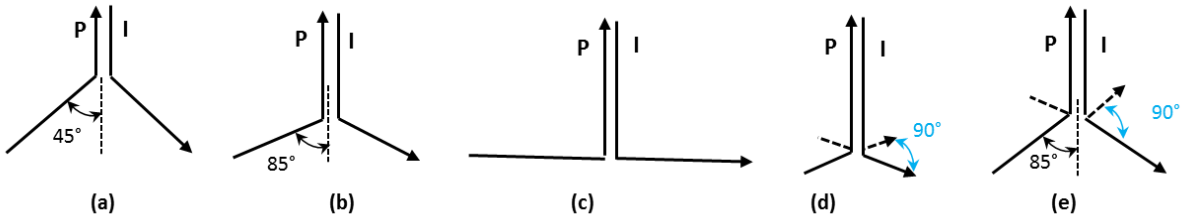


Figure 3: Simulated complex well architectures

(a): "standard" geothermal well with an inclination of 45° relative to the vertical in the reservoir
(b) : sub-horizontal well with an inclination of 85° relative to the vertical in the reservoir
(c) : horizontal drain 1000 m long
(d) : dual horizontal drains 2x500 m long and forming an angle of 90° in the reservoir
(e) : dual sub-horizontal wells (85°) forming an angle of 90° in the reservoir

Table 2: Drilled depths of different well architectures in meters below ground level (mbgl) or in meters drilled (mD)

Well architectures	Case a (standard)	Case b (sub-horizontal)	Case c (horizontal)	Case d (dual horizontal)	Case e (dual sub-horizontal)
Deviation (°)	45	85	90	90	85
Total drains Length (m)	71	574	1000	2x500	2x574
TVD top reservoir (mbgl)	2250	2250	2250	2250	2250
KOP (mbgl)	1263	1475	2275	2275	1475
GBU (°/10m)	1	0.74	-	-	0.74
EOK (mD)	1713	2626	-	-	2626
Average TDD (mD)	2607	3241	3275	3275	5007

2.3 Modelling results

We present the results (Table 3) for the five well architectures modelling cases in terms of:

- the bottom well pressure at both production and injection wells;
- a doublet performance index (DPI) defined as the average ratio of the flowrate with respect to the pressure change in both injection and production wells, expressed in m3/h/bar, i.e. average between the productivity and injectivity index;
- thermal breakthrough at the end of a 30 year injection/production period.

Depending on well architectures, we can observe different behaviours. In the case of "standard" deviated wells (case a), the bottom well pressure vary from 35 bar (production well) to 45 bar (injection well). In the case of sub-horizontal wells (case b), the pressure change due to production or injection is drastically diminished, between 12.5 and 14 bar. In the case of horizontal wells with 1,000 m drain length (case c), the bottom well pressures remain comparable (between 11.4 and 15 bar). Indeed, even if the reservoir-wellbore contact surface is greater in case (c) than in case (b), it can be more advantageous to cross the reservoir thickness directionally rather than to have horizontal wells. Comparable or slightly lower injection or production pressures are obtained when using either two horizontal laterals 500 m in length (case d) or two deviated laterals with an inclination of 85° as in case e.

Table 3: Synthesis of modelling results for the different simulated well architectures

Well architectures	(a)	(b)	(c)	(d)	(e)
Bottom injection pressure (bar)	44.6	14	11.4	12	10.8
Bottom production pressure (bar)	35.3	12.5	15.1	10.8	9.3
Average doublet performance index "DPI" (m3/(h.bar))	5.1	15.1	15.4	17.6	19.9
Production temperature drawdown after 30 years (°C)	1.4	0	0	0	0

The results clearly show a great difference in the performance index according to well architectures. For sub-horizontal wells (case b), the doublet performance is increased by a factor of almost three compared to

the standard directional wells (case a), i.e. 15 m^3/(h.bar) instead of 5 m^3/(h.bar). For the horizontal drains (cases (c) and (d)), the DPI is increased by 3 to 3.5. Lastly, in case (e), with dual sub-horizontal wells, the model gives the best doublet performance with 20 m^3/(h.bar).

For all of the cases modelled, we also calculated the propagation of the cold front and the thermal breakthrough after 30 years of geothermal exploitation. Decrease in production temperature was observed in only one case (standard wells). In all other cases, there is no thermal breakthrough after 30 years.

Numerical modelling shows that in the case of Triassic fluvial sedimentary aquifer with lower or discontinuous permeability, the performance of a geothermal doublet can be increased by using nonstandard well architectures. Nevertheless, the gain obtained must be balanced against the extra costs of these architectures, discussed in chapter 3.

3. COST-PERFORMANCE ANALYSIS

3.1 Cost assessments of modelled well architectures

Drilling cost data for standard directional wells were collected by considering feasibility studies of the most recent operations in Dogger aquifer and the reports required by regulations to support geothermal operating licenses or drilling permits, called PER-DOTEX (Exclusive Exploration Permit – Request for start of Exploration work). These reports are prepared by main project contractors and include detailed information about the doublet design, processing, planning and provisional cost estimates. Effective drilling time and costs are, however, sometimes kept confidential. For this reason, only total cost estimates are used in this work. These include costs of site preparation, mobilization and rigging up, drilling, tripping operations, casing placement, well completion, directional drilling, logging, contingencies and others services and equipment required.

The total cost of drilling standard deviated wells was estimated on the basis of 16 recent deviated doublets drilled or planned during the 2007–2014 period in the Dogger. In order to simplify the cost analysis, no distinction was made between injection and production wells. Doublet cost values in euros were updated to 2014 euro values using the French public works index (TP04: exploratory borings and drillings index). The average total cost for a doublet is estimated to be around $€_{2014}$9.1 million. Unit cost per mD (meter Drilled) is calculated by dividing the total cost by the TDD of the doublet. The unit cost estimates yield a value of €2,263/mD ± €260/mD. Mean deviation reflects relatively low variability (±11.5 %) of drilling cost in the Dogger aquifer, which depends both on the degree of I/P deviation and the TDD. In the Trias, with the same standard directional drilling, it results in a total cost of around $€_{2014}$11.8 million with an average TDD of 5,214 mD (on average 2,607 mD per well; Table 2).

For the sub-horizontal architecture of case (b), operation of only one new doublet (88.3°) was reported from the cost survey in the Dogger formation (Cachan doublet). The PERDOTEX (Socachal et GPC IP, 2014) reported a total investment cost of €12.66 million for a total deviated length of 5,128 mD (average of 2,564 mD per well). The unit cost is calculated at €2,469/mD representing an increase of €206/mD in relation to the previous case (a). Subsequently, for the cost analysis, we assume €2,489/mD as typical unit cost of sub-horizontal well architecture in the study area i.e. an increase of 10% compared to case (a). Thus, considering the figures in Table 2, total costs of sub-horizontal drilling reach €16.2 million in the Trias reservoir.

Estimates for horizontal (case c) and multilateral wells (cases d and e) are difficult to make owing to lack of data. In addition, the drilling technologies used for those architectures may be different from those of directional wells. The additional cost may be mainly due to the extra risk of failure and the technologies involved (Joshi, 2003). The literature review provides some elements of comparison. For instance, the JAS survey showed that horizontal drilling was around 17% more expensive than other options. Also, according to Joshi (2003), horizontal wells cost 1.3 to 2.5 times more than vertical wells. More recently, Husain et al. (2011) have reported that horizontal and multilateral wells drilled for shale field development in the USA prior to 2011 reached slightly over US$5 million per horizontal well and US$11 million per multilateral well. The difference reflects a combination of sometimes radically different drilling conditions and the number of laterals in multilateral drilling.

Alongside the analysis of all data from the literature, the relative extra cost per meter is also of interest to make valid assumptions in the context of the Paris basin. On this basis, the following assumptions are considered and confirmed by expert opinion:

- the extra cost of the horizontal drain (case c) is assumed to be around 2.5% of the cost of the sub-horizontal well (case b) or 12.5% (€283/mD) of the standard well cost;
- the extra cost of dual horizontal drains (case d) is assumed to be close to 17.5% (€396/mD) of the standard well cost;
- the extra cost of the dual sub-horizontal wells of case (e) is assumed to be only 2.5% greater than the cost of case (d) or 20 % (€453/mD) of standard well cost.

Cost assessments for the five cases studied are summarized in Table 4. Depending on drilling architecture, the average cost per mD varies from €2,263/mD (case a) to €2,715/mD (case e). The total investment ranges from €11.80 million to €27.20 million for doublets in the Trias reservoir. These values are calculated using the same vertical depth for

all cases (Table 2) and assuming all other parameters constant, including same drilling conditions.

3.2 Cost-performance analysis

To evaluate the impact of geothermal well architecture on both doublet performance and its cost, a cost-performance ratio or index (CPI) is introduced. CPI assesses the effectiveness of well drilling cost in terms of well productivity and injectivity gained. CPI is therefore calculated as the total annualized doublet cost (TAC) divided by the doublet performance index (DPI):

CPI = TAC / DPI

DPI is obtained from Table 3. TAC (€/year) is calculated with the following equation:

$$TAC = \sum_{t=1}^{T} \frac{TC}{(1+r)^T} = TC \frac{r(1+r)^T}{(1+r)^T - 1}$$

where: TC is the total doublet cost as reported in Table 4; parameter r is the discount rate, assumed equal to 4%; and T is the lifespan of the doublet, usually assumed to be 30 years for geothermal exploitation in the Paris basin.

Table 4 presents the calculated TAC and CPI for the simulated well architectures. Results show that all complex architectures achieve a better cost-performance index when compared with standard directional drilling. A unit of DPI can be estimated between €57k/year and €62k/year (cases b, c and d) while it reaches €75k/year for case (e) and €134k/year for case (a). The relative benefits of complex well architectures are therefore between €55k/year and €77k/year per additional unit of DPI. The highest relative benefits are obtained for sub-horizontal (case b), horizontal or dual-horizontal wells (case c and d).

This finding means that the extra cost of complex architectures compared to standard architecture (45° deviation) can be largely offset by the benefits to the doublet performance index for the same targeted reservoir (i.e. same vertical depth). It also means that the exploitation of a deeper reservoir as the Trias can be economically viable using complex well architectures such as sub-horizontal or horizontal wells.

Table 4: Total doublet cost estimates and cost-performance index (CPI) for different well architectures

Well architectures	**Case a**	**Case b**	**Case c**	**Case d**	**Case e**
Cost estimates basis	16 doublets	1 new doublet	hypothesis	hypothesis	hypothesis
Cost per m (€/mD)	**2263**	**2489**	2546	2659	2715
Extra unit cost (%)	-	10%	12.5%	17.5%	20%
Total doublet cost (M€)	**11.80**	**16.14**	**16.68**	**17.42**	**27.20**
Extra total doublet cost	-	27%	29%	32%	57%
DPI (m^3/(h.bar))	5.1	15.1	15.4	17.6	19.9
TAC (k€/year)	682	933	964	1007	1573
CPI (k€/year per DPI)	**134**	**62**	**62**	**57**	**79**
Relative benefit (k€/year per DPI)	0	72	72	77	55

3.3 Sensitivity analysis of cost-performance index

The lack of data introduces uncertainty into our results. For instance, the cost estimation of sub-horizontal wells was derived from only one planned operation in the study area. The same applies for horizontal and multilateral architectures (cases c, d and e), for which cost estimates were based on assumptions with respect to standard well deviation, i.e. base case (a). However, in the literature highest extra costs of deviated wells are reported with values 1.3 to 2.5 times higher than vertical wells, especially for oil and gas drilling operations in the USA. This can also be true for geothermal operations, as geothermal wells are more expensive than oil and gas wells (larger diameters and higher temperatures). Below, we assume the same range of variation in those extra costs, to analyze their impacts on CPI values. Considering that the cost of standard deviated wells (less than 45°) is 8% higher than vertical wells in the Paris basin, costs of complex architectures can vary from 1.2 to 2.4 times those for standard architectures. Fig. 4 plots the sensitivity analysis of CPI in Trias reservoir.

From Figure 4 it can be seen that the complex architectures yield a better CPI than standard architectures only up to a certain level of relative extra cost. Dual sub-horizontal (case e) architecture becomes economically less efficient if its cost exceeds 2 times the cost of standard architecture, i.e. approximately greater than €4526/mD. The same occurs with sub-horizontal or horizontal architectures (case b and c) when the cost reaches 2.4 times the cost of case (a), i.e. €5974/mD. Nevertheless, such increases should be moderate, as complex well drilling costs should decrease as completion technologies improve and experience is gained from future geothermal operations involving complex well architectures in the study area.

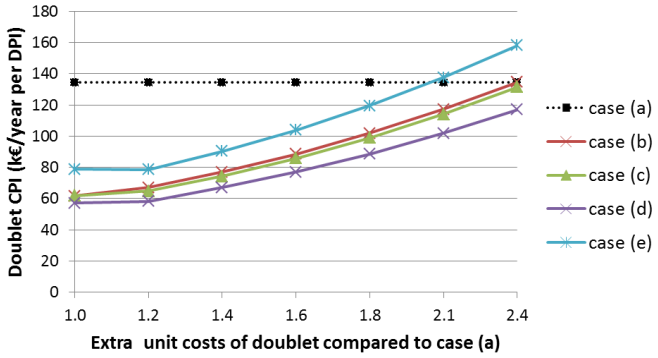


Figure 4: Sensitivity analysis of doublet cost-performance index according to extra cost variation

4. CONCLUSIONS

With progress in complex well architectures and completion technologies, the feasibility of (sub-) horizontal and multilateral wells is being considered seriously for the new generation of geothermal operations in the Paris basin. The implementation of complex well architectures for deep geothermal operations has several advantages such as: (i) access to deeper reservoir units with higher temperature but lower permeability; (ii) improvement in well productivity and injectivity; (iii) probably, less wells for the same heat production. Conversely, there are disadvantages, the main ones being: (i) risks associated with failure in well drilling and/or exploitation and (ii) higher costs compared to standard well architectures.

The work described here is a first quantitative contribution to the establishment of a reliable approach to promote the use of complex geothermal well architectures and ensure successful geothermal operation for a future exploitation of the Triassic sandstones formation. The impact of four well architectures on productivity and injectivity has been considered and compared with standard deviated wells by means of a geothermal modelling framework and an assessment of the doublet performance index (DPI). We have also developed a new cost-performance index (CPI) to evaluate and compare the economic efficiency of complex geothermal wells in the context of Trias geothermal reservoirs in the Paris basin.

Using the model results, the assessment of the doublet performance index (DPI) shows that both productivity and injectivity performance are higher for complex well architectures compared to standard deviated architectures. The highest DPI are obtained for the dual sub-horizontal well architecture (case e), with a DPI of 19.9 m3/(h.bar).

The result of the economic analysis indicates that, despite the higher costs of drilling, complex well architectures yield a better cost-performance index than standard well architectures when targeting the same reservoir. Thus, the additional costs of complex architectures compared to the costs of standard wells are largely offset by the relative benefits of increasing doublet performance index. These benefits are estimated to be between €55k and €77k/year per DPI unit. Moreover, improvements in drilling technologies and further experience from new operations will lead to substantial cost reductions in the future.

APPENDIX A

Nomenclature

General variables

ρ fluid density [kg/m^3]
μ fluid viscosity [Pa.s]
g gravitational acceleration [m/s^2]

Variables used in the well model

r_w wellbore radius [m]
d wellbore diameter [m]
S wellbore cross section [m^2]
$S.dx$ volume element of a well of length dx crossing the reservoir [m^3]
v fluid velocity in the well [m/s]
q_m mass source term in the well [kg/(m^3.s)]
p_w well pressure [Pa]
F_f friction forces [kg/s^2]
f Darcy Weisbach friction factor [-]
ks well roughness [m]
θ well inclination (θ = 0 when horizontal) [deg]
J productivity index describing the outflow or inflow performance of the well [kg/(m.s.Pa)]
α factor including well completion, wellbore skin

Variables used in the reservoir model

k intrinsic reservoir permeability [m^2]
p_r reservoir pressure [Pa]
ω reservoir porosity [-]
u Darcy velocity [m/s]
Q_m mass source term [kg/(m^3.s)]
T reservoir temperature [°C]
ρC_p fluid heat capacity [J/m3/°C]
$(\rho C_p)_{eq}$ equivalent reservoir heat capacity (saturated reservoir rock)
$K_{eq} = \lambda + \delta u$ equivalent conductivity which combines the isotropic conductivity of the porous medium in absence of flow and a term for the dispersivity which is a linear function of the velocity [W/m/°C]

APPENDIX B

Wellbore flow equation

Mass conservation written in discrete form:

$$[\rho_{(x,t+\delta t)} - \rho_{(x,t)}]S\delta x = [(\rho v)_{(x,t)} - (\rho v)_{(x+\delta x,t)}]S\delta t + q_m(x)S\delta x\delta t$$

which in the continuous limit is written:

$$\frac{\partial \rho}{\partial t} + \frac{\partial (\rho v)}{\partial x} = q_m(x)$$

The mass acceleration (momentum conservation) written in discrete form:

$$[(\rho v)_{(x,t+\delta t)} - (\rho v)_{(x,t)}]S\delta x =$$

$$[(\rho v^2)_{(x,t)} - (\rho v^2)_{(x+\delta x,t)}]S\delta t + \left(p_{w(x,t)} - p_{w(x+\delta x,t)}\right)S\delta t - \rho S\delta x g sin\theta \delta t - F_f \delta x \delta t$$

which in the continuous limit is written:

$$\frac{\partial (\rho v)}{\partial t} + \frac{\partial (\rho v^2)}{\partial x} = -\frac{\partial p_w}{\partial x} - \rho g sin\theta - \frac{F_f}{S}$$

Multiplying the mass conservation equation by v and substracting the result from the momentum conservation gives:

$$\boldsymbol{\rho \frac{\partial (v)}{\partial t} + \rho v \frac{\partial (v)}{\partial x} = -v q_m - \frac{\partial p_w}{\partial x} - \rho g sin\theta - \frac{F_f}{S}}$$

Expression of the source term q_m:

We used a formulation similar to that proposed by Dikken (1990) to connect well and reservoir pressures through a linear relation:

$$\boldsymbol{q_m(x) = \frac{J}{S}(p_r(x) - p_w(x))}$$

Furthermore, we assume that there are no inertial/quadratic effects around the well and that the flow from the reservoir into the well is still governed by Darcy's law:

$$q_m(x) = -\frac{1}{S}\int_{\partial S(x)} \frac{\rho k}{\mu}(\nabla p_r + \rho g \nabla z).n$$

Equating both equations, J can be approximated by:

$$J \approx \alpha \frac{k\rho}{\mu}$$

Expression of the friction term F_f for momentum dissipation in the wellbore flow:

The friction term can be expressed using the Darcy-Weisbach friction factor:

$$\frac{F_f}{S} = f\frac{\rho v^2}{4r_w}$$

For laminar flow, the Reynolds number (Re < 2300):

$$f = \frac{64}{Re}$$

$$Re = \frac{\rho v d}{\mu}$$

$$f = \frac{64\mu}{\rho v d} = \frac{32\mu}{\rho v r_w}$$

Finally:

$$\frac{F_f}{S} = \frac{8\mu v}{{r_w}^2}$$

For turbulent flow (Re > 2300):

We can apply Colebrook and White's formula:

$$\frac{1}{\sqrt{f}} = -2log\left(\frac{2.51}{Re\sqrt{f}} + \frac{ks}{3.7d}\right)$$

These two formulas have been implemented in the COMSOL software with a functional dependence on the Reynolds number and therefore well velocity.

Where ρ is constant (fluid incompressible), we can rewrite the mass and momentum conservation equation in the form:

$$\frac{\partial v}{\partial t} + v\frac{\partial v}{\partial x} = -v\frac{q_m}{\rho} - \frac{1}{\rho}\frac{\partial p_w}{\partial x} - gsin\theta - \frac{F_f}{\rho S}$$

$$\frac{\partial v}{\partial t} + 2v\frac{\partial v}{\partial x} = -\frac{1}{\rho}\frac{\partial p_w}{\partial x} - gsin\theta - \frac{F_f}{\rho S}$$

Using Dikken approximation:

$$\frac{\partial v}{\partial t} + 2v\frac{\partial v}{\partial x} = -\frac{1}{\rho}\left[\frac{\partial (p_r)}{\partial x} - \frac{\partial\left(\rho \frac{S}{J}\frac{\partial v}{\partial x}\right)}{\partial x}\right] - gsin\theta - \frac{F_f}{\rho S}$$

$$\boldsymbol{\frac{\partial v}{\partial t} + \frac{\partial v}{\partial x}\left(2v + \frac{S}{J^2}\frac{\partial J}{\partial x}\right) - \frac{S}{J}\frac{\partial^2 v}{\partial x^2} = -\frac{1}{\rho}\frac{\partial p_r}{\partial x} - gsin\theta - f\frac{v^2}{4r_w}}$$

Governing equations for flow and heat transfer in the reservoir

For flow and heat transfer in porous media, the classical Darcy's law and heat transfer modules were applied.

Mass balance is written:

$$\boldsymbol{\frac{\partial (\rho \omega)}{\partial t} + \nabla.(\rho u) = Q_m}$$

with u given by Darcy's law:

$$\boldsymbol{u = -\frac{k}{\mu}(\nabla p_r + \rho g \nabla z)}$$

Heat transfer equation relative to the Darcy velocity is written:

$$\boldsymbol{\left(\rho C_p\right)_{eq}\frac{\partial T}{\partial t} + \rho C_p \nabla.(uT) = \nabla.\left(K_{eq}\nabla T\right) + Q}$$

APPENDIX C

Model boundary conditions

The production and injection wells are modeled by 1D elements crossing the 3D reservoir block. Furthermore, we have defined two 1D models to describe the flow equation in the production and injection wells, as described in Appendix B. The hydraulic and thermal boundary conditions are defined as follows:

a) Hydraulic boundary conditions applied to the 3D porous reservoir:

- A constant hydraulic head (H) at the model limits

$$H(x = \pm 5\ km, y, z) = H(x, y = \pm 4\ km, z) = H_0 = \frac{p_0}{\rho g} + z$$

- A zero flux limit at the top and bottom boundaries of the reservoir:

$$n.\frac{\rho k}{\mu}\nabla p = 0\ at\ z = \pm 25\ m$$

- A mass flux at the well 1D element

$$n.\frac{\rho k}{\mu}\nabla p = J(p_w - p_r)$$

b) Thermal boundary conditions

- A zero conductive heat flux (boundary at the limits of the model – outflow type limit)

$$n.(K\nabla T) = 0$$

- A fixed temperature at the injection well and an outflow boundary condition at the production well which provides a suitable boundary condition for convective heat transfer at outlet boundaries.

For the 1D well model, we applied a Dirichlet boundary condition by imposing the flow velocity at each well extremity:

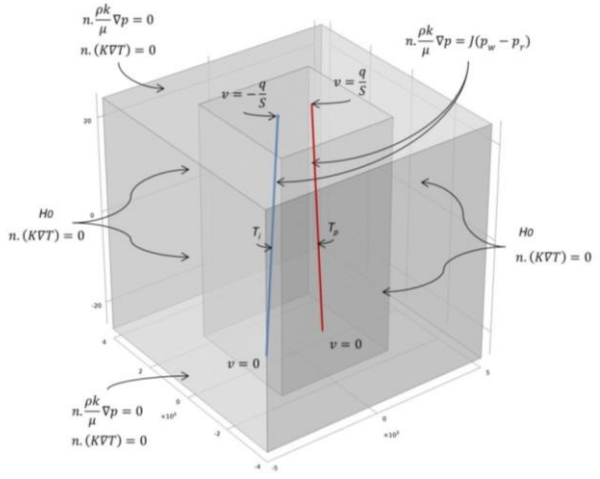
$$v(z = -25) = 0$$

$$v(z = 25) = \pm\frac{q}{S}$$

Where q is the well flowrate [m^3/h]

For the simulations, the flowrate was fixed at 200 m^3/h (average flowrate for geothermal doublet in Paris basin) which then defines the fluid velocity at the well casing shoe. The injection temperature is equal to 40°C.

The initial conditions are uniform hydraulic head and temperature in the 3D porous media and zero velocity at the 1D injection and production wells.



Isoperspective view of the model geometry and boundary conditions

REFERENCES

Amara, M., Capatina L., Lizaik L., 2008. Numerical coupling of 2.5D reservoir and 1.5D wellbore models in order to interpret thermometrics. International Journal of Numerical Methods in Fluids 56-8, 1115-1122.

Boisdet, A., Cautru, J.P., Czernichowski-Lauriol, I., Detoc, S., Foucher, J.C., Fouillac, C.,Honegger, J.L., Martin, J.C., Vuataz, F.D., 1989. Projet Trias, expérimentations en vue de la réinjection de saumures géothermales dans les grès du Trias profond. Report BRGM n◦89 SGN 141 3E/IRG.

Bouchot, V., Bader, A.G., Bialkowski, A., Bonté, D., Bourgine, B., Caritg, S., Castillo,C., Dezayes, C., Gabalda, S., Guillou-Frottier, L., Haffen, S., Hamm, V., Kervévan, C., Lopez, S., Peter-Borie, M., 2012. CLASTIQ-2: Programme de recherche sur les ressources géothermales des réservoirs clastiques en France (bassin de Paris et fossé rhénan). BRGM Report RP-61472-FR, 207 pp.

Chilès, J., Delfiner, P., 1999. Geostatistics: Modeling spatial uncertainty. Wiley, 720 p.

Dikken, Ben J., 1990. Pressure Drop in Horizontal Wells and Its Effect on Production Performance. Society of Petroleum Engineers, November 1990 JPT.

Eschard, R., Lemouzy, P., Bacchiana, C. et al, 1998. "Combining sequence stratigraphy, geostatistical simulations, and production data for modeling a fluvial reservoir in the Chaunoy field (Triassic, France)". AAPG Bulletin, 82- 4, 545-568.

Hadgu, T., Zimmerman, R.W., Bodvarsson, G.S., 1995. Coupled reservoir-wellbore simulation of geothermal reservoir behavior. Geothermics 24- 2, 145-166.

Hamm, V., Lopez, S., 2012. Impact of fluvial sedimentary heterogeneities on heat transfer at a geothermal doublet scale. PROCEEDINGS, Thirty-Seventh Workshop on Geothermal Reservoir Engineering, Stanford University, Stanford, California, January 30 - February 1, 2012. SGP-TR-194

Hill, A.D., Zhu, D., Economides M.J., 2008. Multilateral Wells. Published by Society of Petroleum Engineers, 2008.

Husain T.M., Yeong L.C., Saxena A., Cengiz U., Ketineni S., Khanzhode A., Muhamad H., 2011. Economic comparison of multi-lateral drilling over horizontal Drilling for Marcellus shale field development. Final project report EME 580: Integrative Design of Energy & Mineral Engineering Systems. 131 p.

Joshi, S.D., 1991. Horizontal Well Technology. Published by PennWell, Tulsa Oklahoma, 1991.

Lopez, S., 2003. Modélisation de réservoirs chenalisés méandriformes: approche génétique et stochastique. Thèse de Docteur en Géostatistique. Ecole Nationale Supérieure des Mines de Paris.

Lopez, S., Cojan, I., Rivoirard, J. et al., 2008. Process-based stochastic modeling meandering channelized reservoirs. In: Analogue and numerical modeling of sedimentary systems; from understanding to prediction. Special Publication of the International Association of Sedimentologists, 40, p.139-144. Ed. by Poppe de Boer, et al., Blackwell, Oxford.

Lopez, S., Millot, R., 2008. Problématique de réinjection des fluides géothermiques dans un

réservoir argilo-gréseux: retour d'expériences et apport de l'étude des fluides du Trias du Bassin de Paris. BRGM report RP-56630-FR, 197 pp.

Lopez, S, Hamm, V., Le Brun, M., Schaper, L., Boissier F., Cotiche C., Giuglaris E, 2010. 40 years of Dogger aquifer managment in Ile-de-France, Paris basin, France. Geothermics 39 (2010) 339-356.

Pan, L., Oldenburg C.M., 2013. T2Well-An integrated wellbore-reservoir simulator. Computers & Geosciences, 65, 46-55.

Pan, L., Freifeld, B., Doughty, C., Zakem, S., Sheu, M., Cutright, B., Terrall, T., 2015. Fully coupled wellbore-reservoir modeling of geothermal heat extraction using CO2 as the working fluid. Geothermics 53, 100–113.

Pranter, M. J., Ellison, A. I., Cole, R. D. et al., 2007. Analysis and modeling of intermediate-scale reservoir heterogeneity based on a fluvial point-bar outcrop analog, Williams Fork Formation, Piceance Basin, Colorado. AAPG Bulletin, 91, 1025-1051.

Remoroza, A.I., Moghtaderi, B., Doroodchi, E., 2011. Coupled wellbore and 3Dreservoir simulation of a CO2 EGS. PROCEEDINGS, Thirty-Sixth Workshop on Geothermal Reservoir Engineering, Stanford University, Stanford, California, January 31 - February 2, 2011. SGP-TR-191.

Saeid, S., Al-Khoury, R., Nick, H.M., Barend, F., 2013. An efficient computational model for deep low-enthalpy geothermal systems. Computers & Geosciences 51, 400-409.

Saeid, S., Al-Khoury, R., Nick, H.M., Barend, F., 2014. Experimental-numerical study of heat flow in deep low-enthalpy geothermal conditions. Renewable Energy 62, 716-730.

Socachal et GPC IP, 2014. Demande de Permis de Recherche d'un Gite Géothermique basse Enthalpie – Demande d'ouverture de travaux de forage. PER-DOTEX Report, September 2014.

Acknowledgements

This work was supported by BRGM (French Geological Survey) as part of a 2013–2015 Research Program. We thank DRIEE (Regional and Inter-departmental Direction of the Environment and Energy) and Frederik Bugarel and Louis Hirsinger from CFG Services for their assistance in collecting data and information on geothermal doublets in the Paris basin.